

- (9) Transfer the resulted mixture into crucibles then put the crucibles into a furnace.
- (10) Increase furnace temperature to 300 °C for over a 12 hours period and hold that temperature for 12 hours.
- (11) Increase temperature to 800 °C and hold the temperature for 6 hours before cooling.
- (12) Powder may be heated at 1250 °C for XRD purpose. The temperature of powder treatment is labeled with the XRD pattern.

## 2. Sintering Process

### a) Powder Treatment

step	Rate, °C/minute	Temperature, °C	Dwelling, hour
1	5	1250	6
2	Natural cooling	25	

### b) New Sintering Process of $(La_{0.60}Sr_{0.40})_{0.99}FeO_{3-\delta}$

step	Rate, °C/minute	Temperature, °C	Dwelling
1	0.2	100	2
2	0.2	200	2
3	0.2	300	3
4	0.2	400	5
5	0.5	800	2
6	0.5	1200	6
7	-0.5	700	3
8	-0.5	25	

3. Powder X-ray diffraction measurements were carried on a SINTAG 2000 x-ray diffractometer operating with Cu K $\alpha$ 1 radiation. A stepped scan using a step size of 0.03° was employed.

## Results and Discussion

### X-Ray Diffraction

Previously we concluded that 800 °C might not be sufficient to obtain a single perovskite phase. Specifically Cr doped compositions have a chromate second phase in the powders calcined at 800 °C, which disappears at about 1200 °C. Both Cr and Ti doping help stabilization of the doped perovskite structure for the compositions of interest. However, it is evident that the stability of SrCrO<sub>4</sub> creates problems with obtaining single phase perovskite. Figure 1 shows XRD patterns corresponding to the powders of La<sub>0.19</sub>Sr<sub>0.80</sub>Fe<sub>0.90</sub>Cr<sub>0.10</sub>O<sub>3- $\delta$</sub> , La<sub>0.19</sub>Sr<sub>0.80</sub>Fe<sub>0.80</sub>Cr<sub>0.20</sub>O<sub>3- $\delta$</sub> , La<sub>0.19</sub>Sr<sub>0.80</sub>Fe<sub>0.65</sub>Cr<sub>0.35</sub>O<sub>3- $\delta$</sub> , treated at 1250 °C and furnace cooled. The 35% Cr doping composition has a significant SrCrO<sub>4</sub> second phase, which clearly demonstrates the problem with higher Cr doping. Figure 2 shows XRD patterns corresponding to the powders of

$\text{La}_{0.59}\text{Sr}_{0.40}\text{Fe}_{0.85}\text{Ti}_{0.15}\text{O}_{3-\delta}$ ,  $\text{La}_{0.59}\text{Sr}_{0.40}\text{Fe}_{0.85}\text{Cr}_{0.15}\text{O}_{3-\delta}$ , treated at 1250°C with furnace cooling. While the intensity scale-up indicates some second and/or third phase(s) in these compositions, it appears to be possible to obtain XRD single-phase structures for these compositions. TGA study has shown that perovskite oxides lose oxygen at a higher temperature. Under an atmosphere of lower oxygen partial pressure, they lose even more oxygen, which could be the reason of the second phase formation. A furnace cooling process is far from thermodynamic equilibrium. So a slower cooling process may be required to obtain single-phase perovskite.

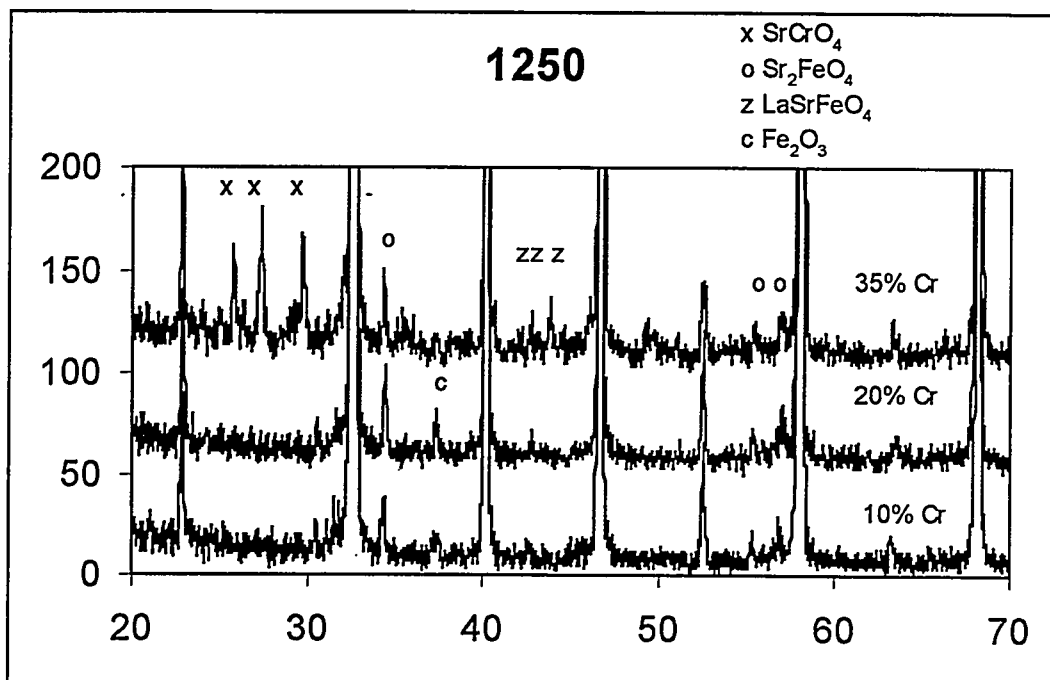


Figure 1. Powder X-Ray Diffraction Patterns taken from 1250 °C heat treatment powders of  $\text{La}_{0.19}\text{Sr}_{0.80}\text{Fe}_{0.90}\text{Cr}_{0.10}\text{O}_{3-\delta}$ ,  $\text{La}_{0.19}\text{Sr}_{0.80}\text{Fe}_{0.80}\text{Cr}_{0.20}\text{O}_{3-\delta}$ ,  $\text{La}_{0.19}\text{Sr}_{0.80}\text{Fe}_{0.65}\text{Cr}_{0.35}\text{O}_{3-\delta}$

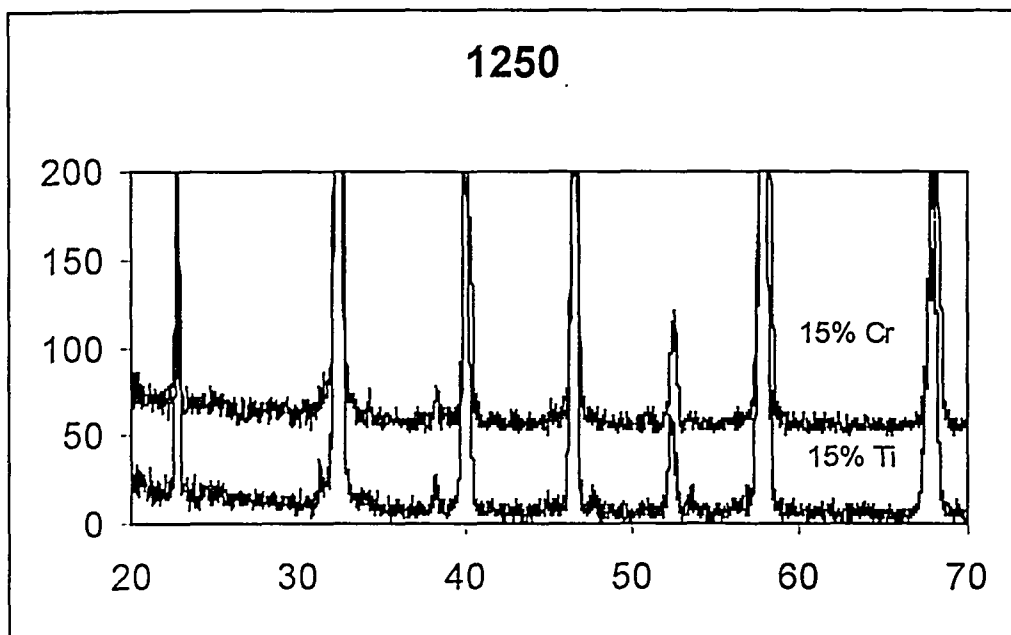


Figure 2. Powder X-Ray Diffraction Patterns taken from 1250 °C heat treatment powders of  $\text{La}_{0.59}\text{Sr}_{0.40}\text{Fe}_{0.85}\text{Ti}_{0.15}\text{O}_{3-\delta}$ ,  $\text{La}_{0.59}\text{Sr}_{0.40}\text{Fe}_{0.85}\text{Cr}_{0.15}\text{O}_{3-\delta}$

Figure 3 shows the XRD patterns of  $(\text{La}_{0.60}\text{Sr}_{0.40})_{0.99}\text{FeO}_{3-\delta}$ , taken from samples prepared through different processes. The lower two patterns are corresponding to powders treated under air with furnace cooling step. While we can see the evidence of  $\text{LaSrFeO}_4$  and/or  $\text{Fe}_2\text{O}_3$  phase(s) in the two patterns, the third pattern of disk sample cooled under nitrogen shows much stronger second and third phases. The top pattern is corresponding to the disk sintered in air by the new slow process, specifically a very slow cooling procedure. This pattern shows no evidence of second phase. All of this clearly suggest that we can process this composition to a dense single phase structure,  $(\text{La}_{0.60}\text{Sr}_{0.40})_{0.99}\text{FeO}_{3-\delta}$ . Figure 4 is the normal XRD pattern of the disk with the composition  $(\text{La}_{0.60}\text{Sr}_{0.40})_{0.99}\text{FeO}_{3-\delta}$  and prepared through the new sintering process.

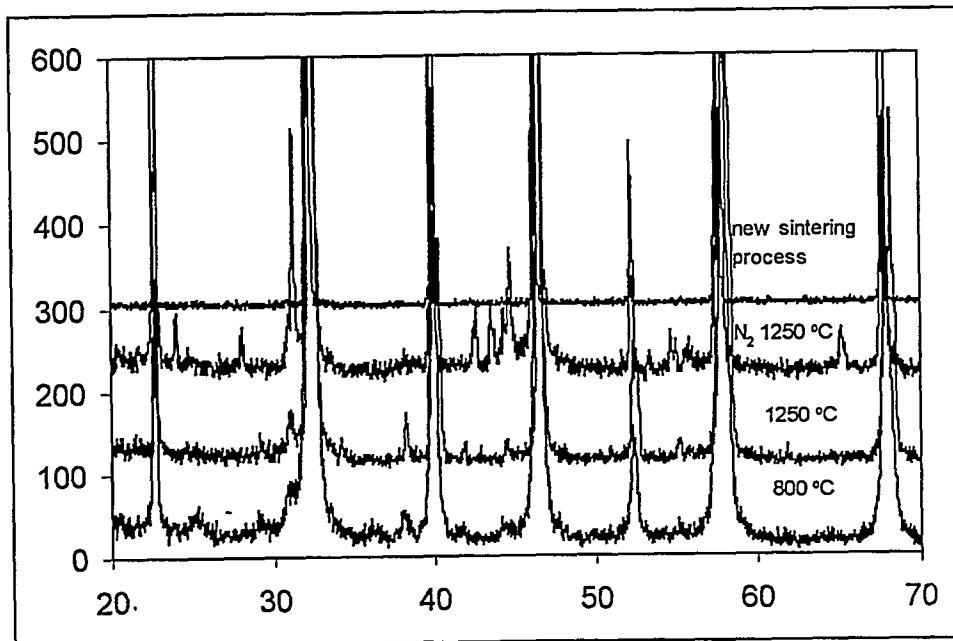


Figure 3. XRD patterns of  $(La_{0.60}Sr_{0.40})_{0.99}FeO_{3-\delta}$

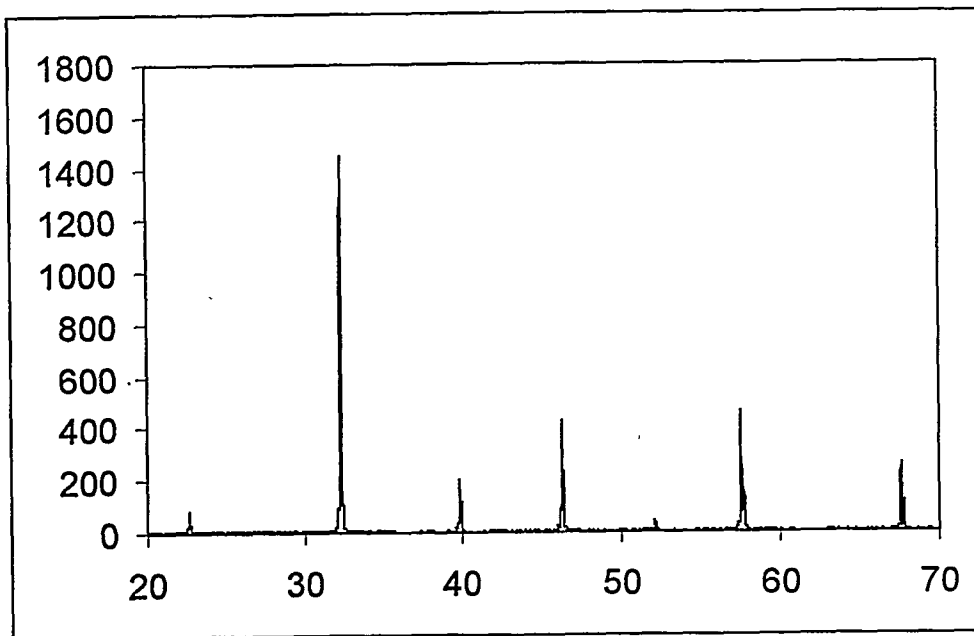


Figure 4. XRD pattern of disk  $(La_{0.60}Sr_{0.40})_{0.99}FeO_{3-\delta}$  by new process

## Stress Analysis

A study on rhombohedral perovskite oxides indicates that applying a stress on a sintered bulk material will result in an orientation change. We applied a stress, 1000 psi for 5 hours on a sintered disk that was prepared by the new sintering process. Figure 5 is the patterns of the disk taken before and after applying the stress. After applying the stress on the disk the splitting peaks intensity ration changed which may reflect the orientation change and the peak shift may reflect a change of angles, lattice parameters. The after stress XRD pattern was taken after the stress was released at least 20 hours, therefore, the lattice parameter change (if any) may be reflected in a stress-strain curve as a part of plastic (ductile) deformation. Figure 6 is a plot of stress-strain, forward-reverse circulation on a sintered disk of  $(La_{0.60}Sr_{0.40})_{0.99}FeO_{3-\delta}$ . Each circle has a plastic deformation (move toward to right). The circles of middle range have larger movement. Figure 7 is a plot of a single cycle stress-strain measurement.

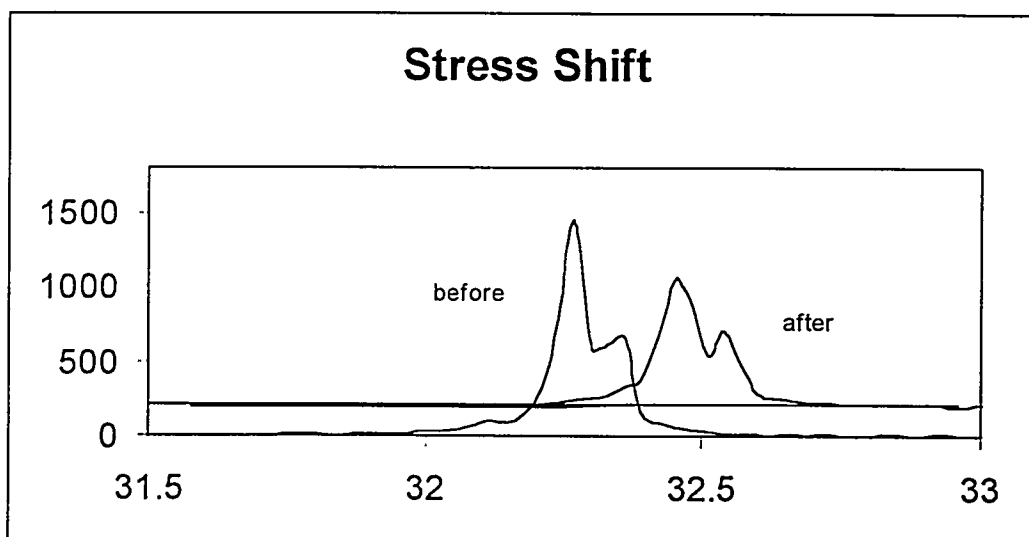


Figure 5. XRD patterns of disk  $(La_{0.60}Sr_{0.40})_{0.99}FeO_{3-\delta}$  before and after stress

LF\_anm cycling 14th July 2000

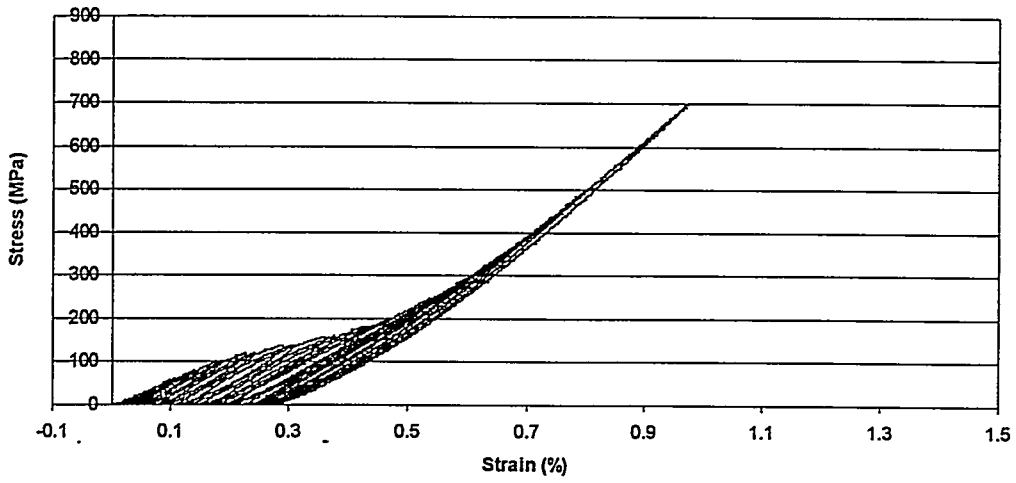


Figure 6. Stress-strain circulation on disk of  $(La_{0.60}Sr_{0.40})_{0.99}FeO_{3-\delta}$

LF\_an\_a 14th July 2000

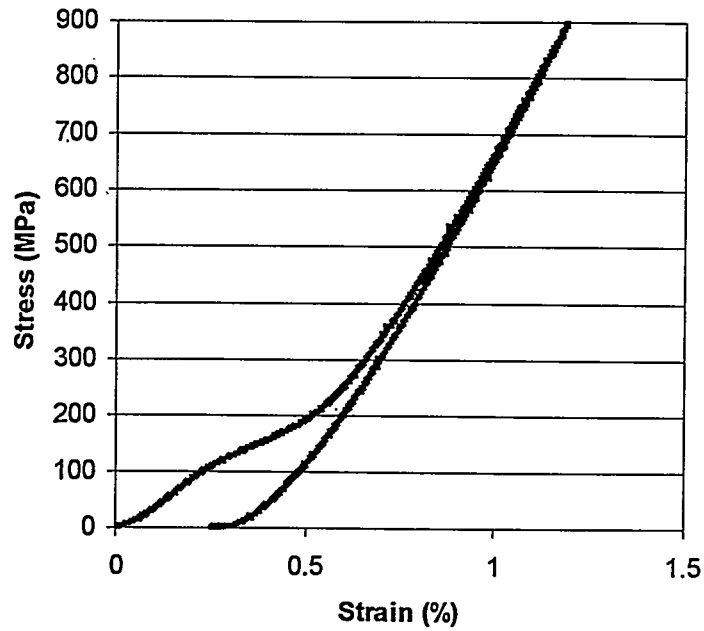


Figure 7. Single forward-reverse stress-strain cycle on disk of  $(La_{0.60}Sr_{0.40})_{0.99}FeO_{3-\delta}$

## Conclusion

- 1) Disks made using  $(\text{La}_{0.60}\text{Sr}_{0.40})_{0.99}\text{FeO}_{3-\delta}$  sintered in air and cooled in nitrogen do not crack during processing, however, these specimens are not single phase structure.
- 2) Disks made using  $(\text{La}_{0.60}\text{Sr}_{0.40})_{0.99}\text{FeO}_{3-\delta}$  sintered in air and "slowly" cooled in air are single phase perovskite, however cracking occurs.
- 3) The addition of either Ti or Cr (5-15%) into the B site of  $(\text{La}_{0.60}\text{Sr}_{0.40})_{0.99}\text{FeO}_{3-\delta}$  tends to allow the formation of single phase perovskite structure. We still are not sure if crack free specimens can be produced in an air atmosphere.

## Program for next quarter

- 1) BP Chemical will complete fabrication of porous  $(\text{La}_{0.60}\text{Sr}_{0.40})_{0.99}\text{FeO}_{3-\delta}$  tubes from PSC powder.
- 2) Provide PSC powder to MIT as required.
- 3) Provide sintered PSC disks to Larson's group at MIT as necessary.
- 4) Provide sintered PSC disks to University of Houston as necessary.
- 5) Provide sintered PSC disks to UIC.
- 6) Initiate studies on Ga perovskite compositions (task 4.2.1.1, and task 4.2.1.2).

## References

1. M. P. Pechini, "Method of Preparing Lead and Alkaline Earth Titanates and Niobates and Coating Method Using the Same to Form a Capacitor," U. S. Pat. No. 3,330,697, 1967.
2. N. G. Eror and H. U. Anderson, "Polymeric Precursor Synthesis of Ceramic Materials"; pp571-77 in Better Ceramics through Chemistry II, Proceedings of Materials Research Society Symposium, Palo Alto, CA, April 1986. Edited by C. J. Brinker, D. E. Clark, and D. R. Ulrich. Materials Research Society, Pittsburgh, PA, 1986.

**TASK 5: Assessment of Microstructure of the Membrane Materials to Evaluate the Effects of vacancy-Impurity Association, defect Clusters, and Vacancy Dopant Association on the Membrane Performance and Stability**

**Professor Niegel Brown  
University of Illinois, Chicago Circle**

Analysis of samples 1 and 2 by scanning transmission electron microscopy is now complete. Differences in microstructures are observed for the samples prepared under different conditions and with different compositions. Work is continuing to analyze the data and compare with the transport measurements to infer the effect of microstructure on the properties.

**Task 6: Measurement of Surface Activation/Reaction rates in Ion Transport Membranes using Isotope Tracer and Transient Kinetic Techniques.**

**Prof. Alan Jacobson, University of Houston/University of Toronto**

**Progress during past 3 months at the University of Toronto**

(1) Oxygen isotope infusion under gradientless conditions.

As planned, the initial set of oxygen infusions were carried out during the current quarter, and the resulting profiles analyzed to extract values of  $k_O$  and  $D_O$ , the surface exchange coefficient and bulk diffusion coefficient respectively, for oxygen in two ferrite materials. The following table summarizes the materials, the conditions for the infusions and the derived transport parameters.

Materials Studied	T(C)	Oxygen activity (* assume WGS eq.)	$D_O / \text{cm}^2 \text{ s}^{-1}$	$k_O / \text{cm s}^{-1}$ (* not redox)
$\text{La}_{0.2}\text{Sr}_{0.8}\text{FeO}_{3-x}$	850	0.2	$5.6 \times 10^{-7}$	$9 \times 10^{-6}$
$\text{La}_{0.2}\text{Sr}_{0.8}\text{FeO}_{3-x}$	750	0.2	$1.3 \times 10^{-7}$	$4.8 \times 10^{-6}$
$\text{La}_{0.2}\text{Sr}_{0.8}\text{FeO}_{3-x}$	850	$10^{-16}^*$	$<9 \times 10^{-7}$	$>8 \times 10^{-6}^*$
$\text{La}_{0.2}\text{Sr}_{0.8}\text{Fe}_{0.8}\text{Cr}_{0.2}\text{O}_{3-x}$	850	0.2	$9 \times 10^{-7}$	$4 \times 10^{-5}$
$\text{La}_{0.2}\text{Sr}_{0.8}\text{Fe}_{0.8}\text{Cr}_{0.2}\text{O}_{3-x}$	750	0.2	$2.1 \times 10^{-7}$	$1.6 \times 10^{-5}$
$\text{La}_{0.2}\text{Sr}_{0.8}\text{Fe}_{0.8}\text{Cr}_{0.2}\text{O}_{3-x}$	750	$10^{-17}^*$	N/A	N/A



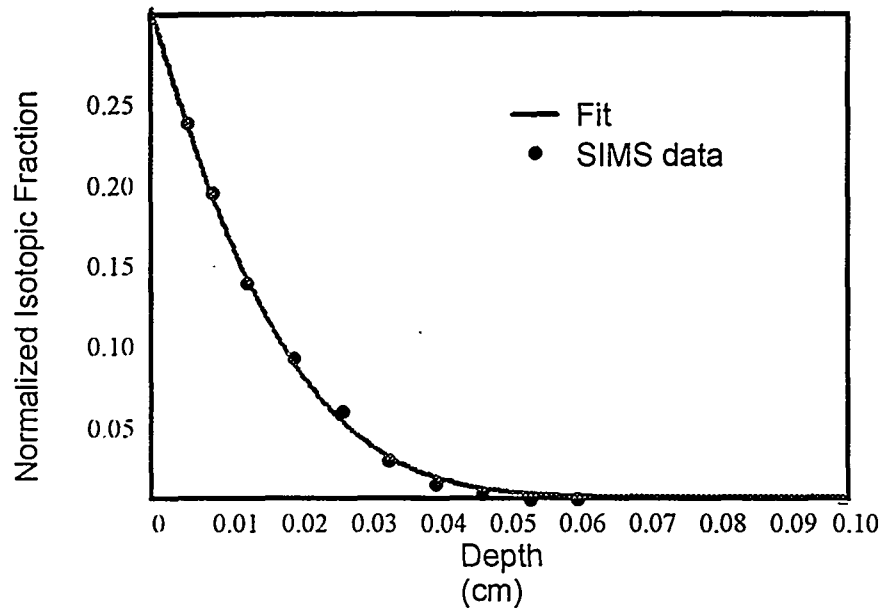


Fig 1 A typical  $^{18}\text{O}$  profile and the fit to the data giving  $D_{\text{O}}$  and  $k_{\text{O}}$

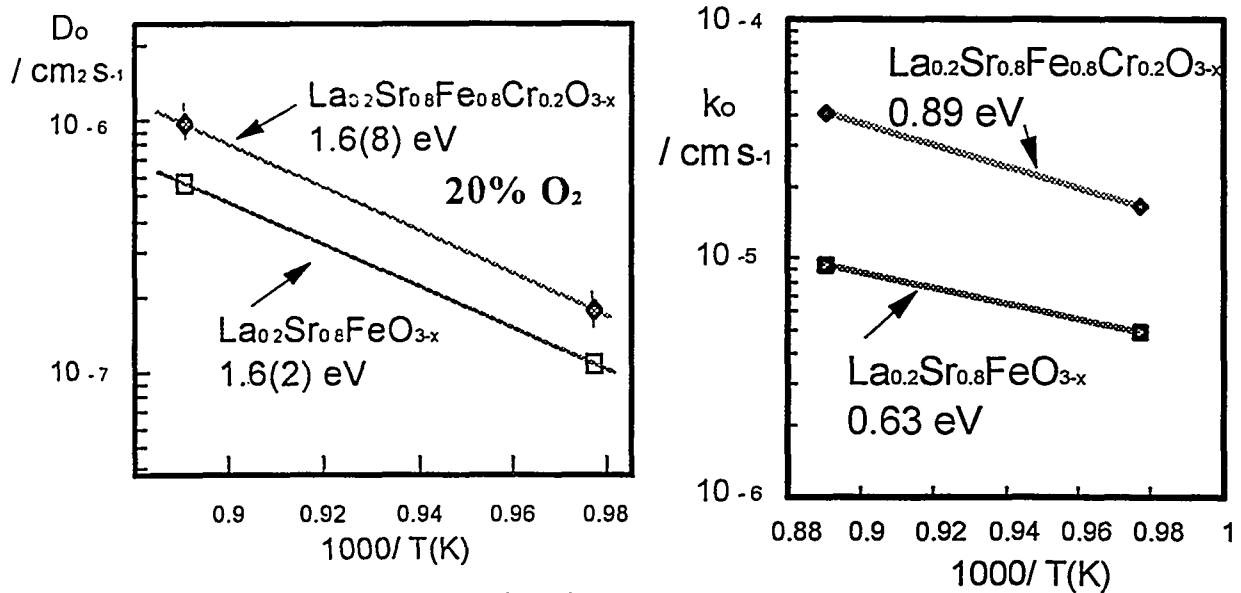


Fig.2. Values of  $D_{\text{O}}$  and  $k_{\text{O}}$  determined by

SIMS analysis  $^{18}\text{O}$  isotope profiles

The  $\text{La}_{0.2}\text{Sr}_{0.8}\text{FeO}_{3-x}$  material was prepared by the U. Missouri group and the  $\text{La}_{0.2}\text{Sr}_{0.8}\text{Fe}_{0.8}\text{Cr}_{0.2}\text{O}_{3-x}$  material from Praxair Specialty Ceramics. Infusions in 20% oxygen atmosphere were performed at the two temperatures for both materials. One of the resulting  $^{18}\text{O}$  profiles is shown in Figure 1. Also shown in the Figure is the simulated profile generated using the derived values of  $k_{\text{O}}$  and  $D_{\text{O}}$ . These values were derived from the simple 1-D diffusion equation solution assuming constant gas phase isotopic composition. This condition was

essentially true for the oxygen atmospheres, but not for the reducing atmospheres (see below) Figures 2 and 3 show Arrhenius plots of the derived values of  $k_O$  and  $D_O$ , for these materials infused in air. In order to compare these values to those obtained in conductivity relaxation experiments, and to calculate the vacancy diffusion coefficient,  $D_v$ , from the derived values of  $D_O$ , requires currently unavailable information about the vacancy concentrations at the infusion conditions is required. With reasonable assumptions about the vacancy concentrations, the values above agree with the conductivity relaxation results obtained at the University of Houston. Preliminary infusions were also made in atmospheres characteristic of the fuel side of a methane partial oxidation membrane. In these cases, the gas atmosphere was  $C^{18}O_2:H_2:Ar$  (proportions 5:5:90). Unless equilibrium in the water-gas-shift (WGS) reaction is established, the oxygen potential is undefined for this mixture and the oxidation state of the material is controlled by the dynamic balance between reduction by hydrogen (and some CO) and oxidation by  $CO_2$  (and some  $H_2O$ ). The conversion in the reverse WGS reaction was monitored during the experiment and did not reach equilibrium. At the 1 Aug meeting, the WGS equilibrium was erroneously reported to be achieved, but in fact only 10% conversion of the  $CO_2:H_2$  mixture to equilibrium was achieved in the  $750^\circ C$  experiment. Further complications arise from the extremely rapid surface exchange of  $CO_2$  with the surface. This has been reported for other oxides. Rapid exchange is advantageous in that it assures that sufficient oxygen is infused for proper measurement of the diffusion coefficient. However, this exchange process, which presumably takes place through a carbonate intermediate does not represent a redox process involved in net oxygen transport across the surface. The value of  $k_o$  reported in the table corresponds to the exchange mechanism and is not necessarily relevant to membrane operation. The rate of the reverse WGS reaction gives some indication of the rate of the redox process and its equivalent will be used in the future. An additional complication arising from the extremely rapid exchange is that the gas phase isotopic composition is not constant during the experiment. Therefore the nominal analysis based on a constant isotope fraction gives false values. The values indicated in the table for these experiments are limits based on the nominal values and a semiquantitative interpretation of the effects of the changing gas composition. A full simulation with a changing gas composition is required to obtain the best values of  $D_O$  and will be done during the next quarter.

## (2) Transient oxygen isotope infusion in operating membrane reactors.

All the parts for the membrane reactor have been received and initial assembly and shakedown of the reactor is currently underway. As described in the previous report, the membrane reactor is a tubular design, rather than the initial design to use disc-shaped membranes. Tension is held on the seals by a bellows fitting at the end of the reactor. We have been delayed by the discovery this summer that the existing Hasteloy outer tube which forms part of our reactor system and which was to contain the membrane assembly had been distorted by improper mounting which resulted in bending by thermal expansion forces at high temperature. We received its replacement from the shop during August. Initial tubular samples of  $La_{0.6}Sr_{0.4}Fe_{0.8}Co_{0.2}O_{3-x}$  have been received from Professor Jacobson's group during the past three months and will be the first materials tested in the reactor.

## Progress during the last 3 months at UH

Electrical conductivity relaxation.

We have continued electrical conductivity relaxation measurements to obtain values of  $D$  and  $k$  to guide the infusion studies. The new apparatus has a much faster switching time (300msec). We are also using a lock-in amplifier ac technique in order to measure very small changes in the resistance of the sample. This method permits data acquisition over a wider range of pressure switches on the same sample and measurements with only small departures from equilibrium.

The specific compositions that have been measured are shown in the table. Of these, we will remeasure  $\text{La}_{0.2}\text{Sr}_{0.8}\text{FeO}_{3-x}$  because of some discrepancies in the results and we will complete the measurements on  $\text{La}_{0.2}\text{Sr}_{0.8}\text{Fe}_{0.8}\text{Cr}_{0.2}\text{O}_{3-x}$ . The results for the four systems completed to date are shown in the figures below for both  $D$  and  $k$

$\text{La}_{0.2}\text{Sr}_{0.8}\text{FeO}_{3-x}$
$\text{La}_{0.2}\text{Sr}_{0.8}\text{Fe}_{0.8}\text{Cr}_{0.2}\text{O}_{3-x}$
$\text{La}_{0.5}\text{Sr}_{0.5}\text{FeO}_{3-x}$
$\text{La}_{0.5}\text{Sr}_{0.5}\text{Fe}_{0.8}\text{Ga}_{0.2}\text{O}_{3-x}$
$\text{La}_{0.6}\text{Sr}_{0.4}\text{Fe}_{0.8}\text{Co}_{0.2}\text{O}_{3-x}$

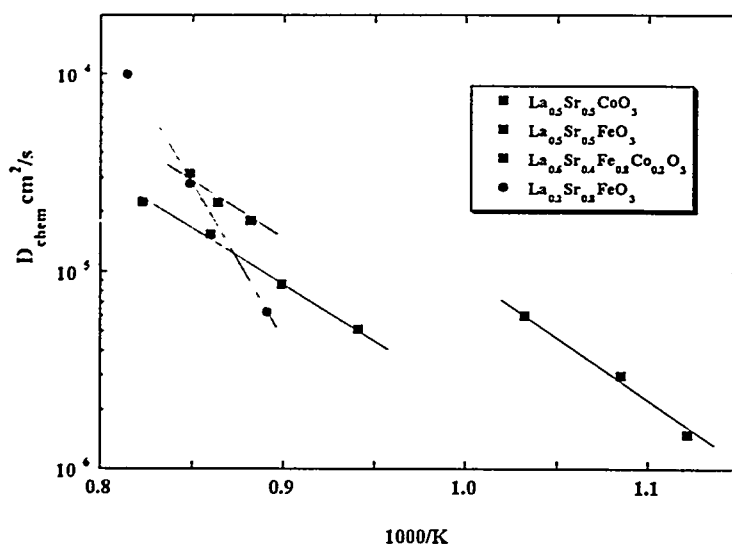


Figure 3 Comparison of  $D_{\text{chem}}$  values measured by electrical conductivity relaxation.

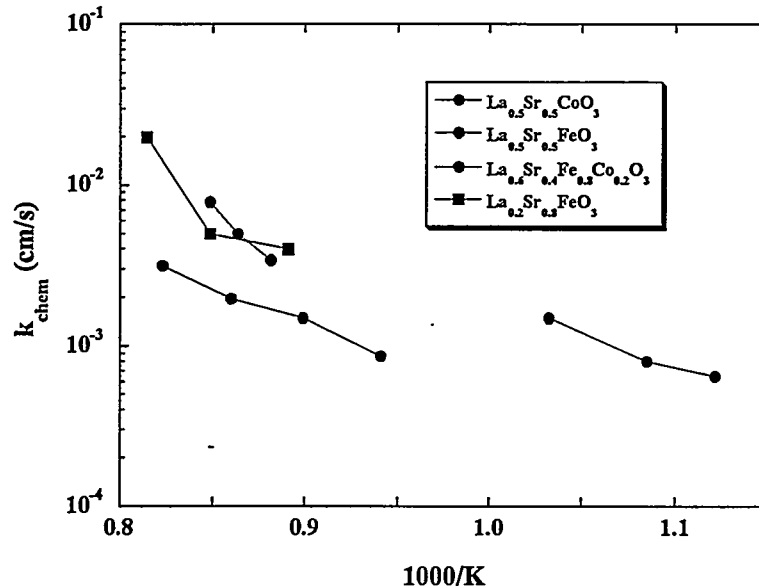


Figure 4 Comparison of  $k_{\text{chem}}$  values measured by electrical conductivity relaxation.

In both sets of data, the results for  $\text{La}_{0.2}\text{Sr}_{0.8}\text{FeO}_{3-x}$  are anomalous and will be remeasured. The results show that the addition of cobalt increases both  $D$  and  $k$  relative to iron as anticipated from previous data

In order to carry out the isotope transient/membrane experiments at UT, we need to fabricate tubes of the appropriate dimensions. We will, for the present, use  $\text{La}_{0.6}\text{Sr}_{0.4}\text{Fe}_{0.8}\text{Co}_{0.2}\text{O}_{3-x}$  as the material. We used the sintering protocol that we have developed to fabricate suitable rods. Attempts to machine the sintered rods to form tubes were not successful. Two alternatives were proposed. In the first, cold isostatic pressing is used to directly form the green tube, which is then sintered. Second, a green rod is partially sintered and then machined. We have evaluated the former route and found that it can be used successfully to make tubes of the appropriate dimensions. In the figure below is a representative example of a tube isostatically pressed and sintered is shown. The outside diameter is 6mm and the wall thickness is 0.5mm. Approximately 1 cm sections of this tube will be cut and mounted in the permeation apparatus at UT.

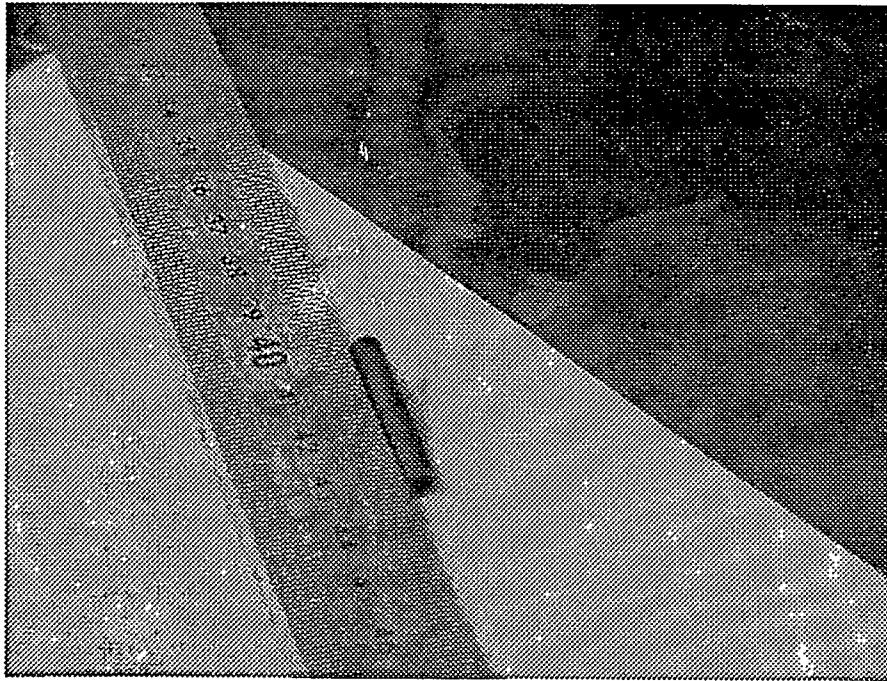


Fig. 5 Sintered tube of  $\text{La}_{0.6}\text{Sr}_{0.4}\text{Fe}_{0.8}\text{Co}_{0.2}\text{O}_{3-x}$  for use in isotopic transient measurements.

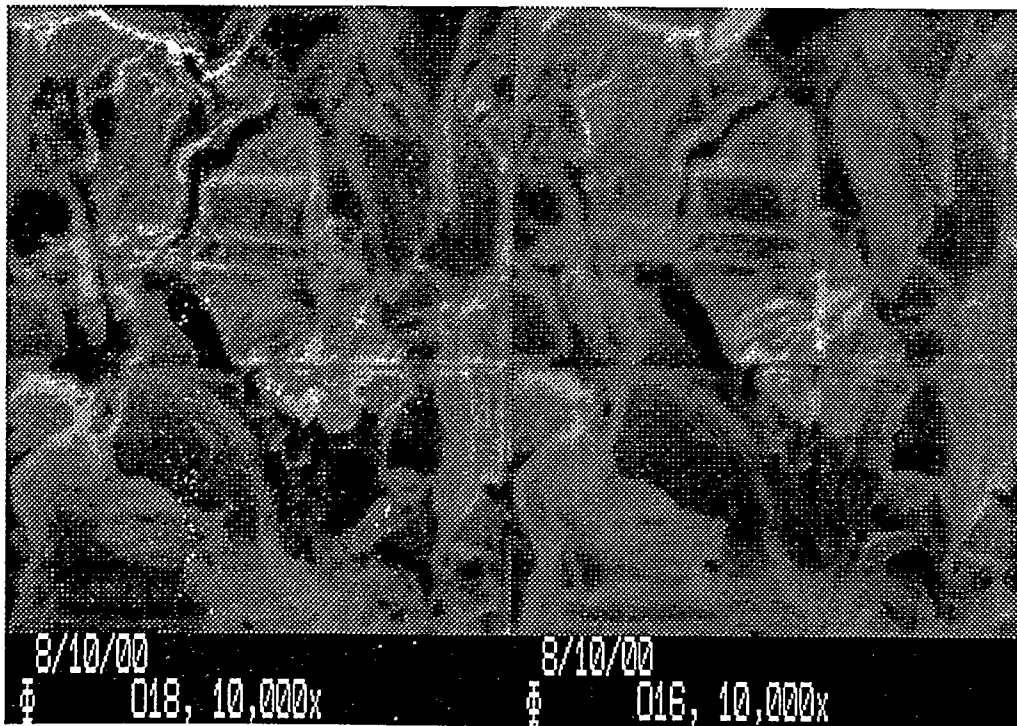


Fig 6 O18 and O16 SIMS images of a polyphasic ceramic to illustrate the resolution

The gallium source for the SIMS instrument has been delivered and installed. This gallium

source will provide higher resolution in-depth profiling than currently available. The software and resolution capability are being evaluated. The images below are the O16 and O18 images of a multiphase sample that was used as a reference for the resolution. The figures are 20 mm by 30 mm and indicate sub-micron resolution.

#### **DOE Tasks for next 3 months University of Houston**

- (1) We will continue the electrical conductivity relaxation measurements on  $\text{La}_{0.2}\text{Sr}_{0.8}\text{FeO}_3$  to resolve the observed anomaly and complete the measurements on  $\text{La}_{0.2}\text{Sr}_{0.8}\text{Fe}_{0.8}\text{Cr}_{0.2}\text{O}_{3-x}$ .
- (2) Additional tubular and disk samples of  $\text{La}_{0.2}\text{Sr}_{0.8}\text{Cr}_{0.2}\text{O}_{3-x}$  will be prepared for transient membrane studies and isotope infusion.
- (3) The commissioning of gallium source for the SIMS instrument will be completed and used for higher resolution isotope depth profiles.
- (4)

#### **DOE Tasks for next 3 months University of Toronto.**

- (1)  $^{18}\text{O}$  infusion in ferrites in gradientless conditions.
  - (a) The analysis of the profiles obtained in this quarter will be completed, including simulations with changing gas composition to obtain the best values of the transport parameters. One of the profiles also remains unmeasured ( $750^\circ\text{C}$  reducing atmosphere infusion for in  $\text{CO}_2/\text{H}_2$ ) and will be analyzed.
  - (b) Further examinations of the oxygen transport in  $\text{La}_{0.2}\text{Sr}_{0.8}\text{FeO}_{3-x}$  and  $\text{La}_{0.2}\text{Sr}_{0.8}\text{Fe}_{0.8}\text{Cr}_{0.2}\text{O}_{3-x}$  under reducing conditions will be performed. We will use  $\text{C}^*\text{O}_2/\text{CO}$  mixtures for the infusion, thus establishing a defined oxygen potential, but allowing measurement of the redox process by being able to follow the extent of isotopic equilibration between CO and  $\text{CO}_2$  in the mass spectrometer.
  - (c) Additional infusions in air will be performed to extend the temperature range on the ferrites above and repeat several of the conditions.
  - (d) After these, time permitting, we will perform infusion measurements on an additional composition, either  $\text{La}_{0.6}\text{Sr}_{0.4}\text{Fe}_{0.8}\text{Co}_{0.2}\text{O}_{3-x}$  or  $\text{La}_{0.6}\text{Sr}_{0.4}\text{FeO}_3$  at the standard conditions above.
- (2) Operating membrane experiments
  - (a) The initial shake-down experiments will proceed as before. The initial assembly will use a dense alumina or quartz tube in place of the membrane. This will allow shakedown of the system without risking the perovskite tubes and proved rigorous leak-check to validate the seals. If all goes well, we will then start oxygen permeation measurements (with no reductant on the fuel side) towards the end of the period with the  $\text{La}_{0.6}\text{Sr}_{0.4}\text{Fe}_{0.8}\text{Co}_{0.2}\text{O}_{3-x}$  tube currently available.